Final Draft
of the original manuscript:

Rangou, S.; Buhr, K.; Filiz, V.; Clodt, J.I.; Lademann, B.; Hahn, J.;
Jung, A.; Abetz, V.:

Self-organized isoporous membranes with tailored pore sizes

In: Journal of Membrane Science (2013) Elsevier

DOI: 10.1016/j.memsci.2013.10.015

Self-organized isoporous membranes with tailored pore sizes

Sofia Rangou[1], Kristian Buhr[1], Volkan Filiz[1], Juliana Isabel Clodt[1], Brigitte Lademann[1], Janina Hahn[1], Adina Jung[1] and Volker Abetz[1,2]*

[1] *Helmholtz-Zentrum Geesthacht, Institute of Polymer Research*

Max-Planck-Str.1, 21502 Geesthacht, Germany

[2] *University of Hamburg, Institute of Physical Chemistry*

Grindelallee 117, 20146 Hamburg, Germany

** Prof. Dr. V. Abetz (Corresponding Author),*

e-mail: volker.abetz@hzg.de

Tel: +49 4152 872461

Fax: +49 4152 872499

Abstract

Membrane formation via the combination of self-assembly and the non-solvent induced phase separation (NIPS) process of diblock copolymers is investigated. Several polystyrene-*block*-poly(4-vinylpyridine) (PS-*b*-P4VP) diblock copolymers with different molecular weights and weight percentages of both blocks are tested under different parameters, leading to membrane surfaces with uniform pores of approximately 20-70 nm diameter. The average pore diameter is proved to be adjustable by changing the total molar mass of the block copolymer. The solution composition is an additional parameter controlling the structure formation. The purpose was to explore the limits of the membrane structure formation and find upper and lower limits since the molecular weight and the composition of this diblock cpolymer. Scanning electron microscopy (SEM) is used to image the surface morphology and the homogeneity of the pore sizes. Primary results of water flux and retention are presented.

Keywords: amphiphilic diblock copolymers; isoporous membranes; self-assembly; tailored pore size

1. Introduction

The need of separation processes based on membranes with defined pore sizes has greatly increased in the past decades. In this direction block copolymers are considered to be the most promising candidates[1] due to their ability to self-assemble into defined morphologies.[2] They offer a variety of nanostructures leading to membranes with controlled pore

dimensions.[3] [4] The pore dimension could be influenced through several procedures after or during the membrane formation like track etching[5], selective removal[6] of one of the components or phase inversion.[7] Especially amphiphilic block copolymers, due to the incompatibility of their segments in selective solvents, are able to self-organize into micelles or vesicles.[8] Many applications arose from these materials e.g. in nanolithography, drug delivery, and especially separation technologies.[9-21] This has led to numerous approaches to achieve homogeneous regular porous membranes.[22-25] Among possible membrane structures, the formation of an integral asymmetric structure with a well-organized, isoporous surface layer supported by a sponge-like substructure is of special interest. It can be prepared in one step by dipping the block copolymer solution after film casting into a precipitation bath. This leads to fast formation of a stable and selective membrane layer. The mesoscopic porous structure is a result of both the microphase separation tendency of the block copolymer and the macrophase separation induced from the still dissolved block copolymer areas by the solvent – non solvent exchange.

Polystyrene-*b*-poly(4-vinylpyridine) (PS-*b*-P4VP) was the first polymer under investigation to create integral asymmetric membranes with highly uniform pore sizes.[23] Since then several publications based on this specific block copolymer system have appeared.[26-32] Also the first studies on the formation of isoporous hollow fibre membranes using the NIPS process have been reported. [33] The highly ordered morphologies that are required for efficient separation are under investigation in terms of reduction of the expensive block copolymer used for the formation of the membrane. This can be achieved by reducing the polymer concentration in the casting solution and keeping the viscosity sufficiently large by additives.[28, 30, 31, 34] Block copolymer membranes are promising separation devices for controlling the diffusion of molecules with different sizes as presented in the work of Yang et al. over a long time without fouling.[35] The selection of an appropriate block copolymer for these membranes offered enhanced mechanical properties as well.[35] This work could be considered as a prototype of fine tuning of the membrane properties based on the chosen block copolymers allowing the fabrication of membranes with improved chemical, mechanical and biological tolerance. Recently triblock terpolymers are explored for membrane applications. [36, 37] Triblock terpolymers offer an extended tunability and more reliable self-assembly, compared to their diblock copolymer counterparts.[37]

Since a membrane layer is an interphase between adjacent phases, acting as a selective barrier, the pore homogeneity and uniformity play a crucial role in regulating the transport between the two parts making them ideal for macromolecular separations, hemodialysis,

micro/nanofluidics, and water filtration.[38, 39] Adjusting pore sizes by varying the molecular weight and the block copolymer composition was our goal in this work. Therefore, the phase inversion method was combined with the self-assembly of a variety of PS-*b*-P4VP block copolymers to achieve membranes with high porosity and uniform pore sizes.

2. Experimental Section

2.1 Polymer Synthesis

Tetrahydrofuran (THF) and *N*,*N*-dimethylformamide (DMF) were ordered from Th. Geyer. Styrene, 4-vinylpyridine (4VP), ethylaluminium dichloride (1M in hexane) and sec-butyllithium (*sec*-BuLi) were purchased from Sigma-Aldrich. THF was purified by successive distillation from potassium under argon atmosphere. Styrene was treated with dibutylmagnesium ($MgBu_2$) and freshly distilled prior to use. 4VP was distilled under reduced pressure and stored over calcium hydride (CaH_2) and distilled again after treating twice with ethylaluminium dichloride. PS-*b*-P4VP was synthesized via sequential anionic polymerization at -67°C in THF. The polymerization of styrene was initiated by *sec*-BuLi. After 2 h 4VP was added via a syringe and the solution was stirred for further 4 h. The polymerization was quenched with methanol. After removal of THF under reduced pressure the polymer was precipitated into water. The polymer precipitated quantitatively, was filtered and dried in vacuum until constant weight.

2.2 Characterization Techniques

Molar masses and polydispersities of the polystyrene precursors and the block copolymers were determined by size exclusion chromatography (SEC). The molecular weights of the block copolymers were obtained from the molecular weight of polystyrene precursor combined with the results of the block copolymer composition as obtained from ^{1}H-NMR spectroscopy using tetramethylsilane (TMS) as a reference on a Bruker AV-300. SEC measurements were performed at 50°C in dimethylacetamide (DMAc) using 3μ PSS SDV gel columns at a flow rate of 1.0 mL min^{-1} (VWR-Hitachi 2130 pump). A Waters 2410 refractive-index detector (λ=930 nm) with a PS calibration was used.

Scanning electron microscopy (SEM) was carried out on a LEO Gemini 1550 VP at a voltage of 3-5 kV. Samples were sputtered with 2 nm Pt. Cross-sections were prepared under cryogenic conditions. Pore size distributions were determined using the software analySIS (Olympus) on basis of the SEM results. The viscosities of block copolymer solutions were

measured with a RC20 cone and plate viscometer from Rheotec at 20 °C and a shear rate of 500/s.

Water flux and retention measurements were performed in dead-end mode using a home-made automatic testing device at trans-membrane pressures 2.0 to 2.3 bar at room temperature. The volume was measured every 15 min over a balance and pressure was measured as well. The effective membrane area was 1.77 cm^2. These studies were conducted employing demineralized water with an electrical conductivity of ≈0.055 $\mu S \cdot cm^{-1}$.

2.3 Membrane Preparation

The different block copolymers were dissolved in a THF/DMF mixture to gain concentrations ranging from 19 to 35 wt %. The solvent composition was also varied according to the total molecular weight and the weight percentage of the P4VP block in the block copolymer. After stirring for 48 hours the solution was directly cast by a home-made casting machine using a doctor blade with a gap height adjusted to 200 μm on a polyester nonwoven support. The evaporation time before immersion into a water bath with a constant temperature of 20 °C was varied until the best results (highest pore uniformity) was observed. On the casting machine the speed of the take-up reel are adjustable in order to control the evaporation time before immersing the solution cast film into the non-solvent bath. Compared to manual casting, machine casting leads to a good reproducibility of the membranes. After leaving the cast membranes in a water bath for 20 minutes, the membranes were dried 2 days under vacuum at 60 °C to remove all residual solvents. The thermal stability of the PS-*b*-P4VP block copolymer membranes up to 110 °C has been proven in a previous work.[25]

3. Results and Discussion

The aim of this work was the development and optimization of the hexagonally packed pore structures on membrane surfaces from amphiphilic PS-*b*-P4VP block copolymers. Therefore different molecular weights and compositions were chosen and the influence of the solvent mixture composition, casting conditions, and viscosity of the polymeric solution were investigated. The membranes are formed through the phase inversion process. First a polymeric solution is cast on a non-woven support. Then the resulting solution film is exposed to the surrounding atmosphere (typically air at room temperature) allowing the solvent(s) to partly evaporate. The evaporation leads to the formation of a concentration gradient of the solvent perpendicular to the surface. During this time microphase separation occurs at the surface due to the immiscibility of the blocks.[40] In this case of a cylindrical

polystyrene-*block*-poly(ethylene oxide) diblock copolymer a fast evaporating solvent (benzene) was studied and the microphase separation propagated perpendicular from the surface towards the substrate. However, there are two extreme orientations for an anisotropic microphase morphology possible. Lamellae or cylinders can be aligned parallel or perpendicular to the surface. In situations, where the film thickness is very large in comparison to the typical chain dimensions, the influence of the substrate on the orientation at the surface can be neglected. The segregation strength between the different polymer blocks and the relaxation rate of the block copolymer chains follow different functions with respect to the concentration. [39] Therefore the concentration gradient of the solvent together with the relaxation rate and the repulsion between the blocks are crucial parameters influencing the orientation of the propagating microphase separation, when drying a film of a block copolymer solution. Phillip at al. found that a faster evaporation of the solvent leads to a strong concentration gradient and the mcrophase separation propagates perpendicular to the surface, resulting in perpendicular aligned cylinders in a polystyrene-*block*-polylactide diblock copolymer. When the evaporation accours more slowly, a parallel alignment of the cylinders is more pronounced.[39] The use of solvent mixtures rather than pure solvents and the kinetic interference of a quenching process during structure formation lead to additional parameters which can be used to control the structure formation of the final membrane. Also the question, if the block copolymer solution before casting represents a homogenous phase or a micellar solution may be important.. The quenching happens by transferring the evaporating film into a precipitant bath for the polymer. Here the exchange of the solvent / non-solvent of the polymeric solution is occurring. These aspects will be examined separately on their influence to the final porous structure.

3.1 Block Copolymer Characterization

As mentioned before, the block copolymers were characterized by size exclusion chromatography (SEC) and ^{1}H-NMR. The block copolymer total molecular weight ranged from 100 000 g/mol up to 330 000 g/mol with P4VP compositions from 9 wt % up to 26.6 wt %. The molecular characteristics of all polymers are listed in **Table 1**. For this work it was also useful to predict the morphological tendency of the diblock copolymers in bulk (after the thermodynamic equilibrium is reached through the slow solvent evaporation and annealing of the films) since careful selection of the block copolymer parameters was required to reach our target. All block copolymers have rather similar compositions in the region wherein P4VP is expected to form spherical or cylindrical domains in the bulk. The value of the Flory-Huggins

interaction parameter between PS and P4VP is on the order of $\chi_{S,4VP} = 0.35$. [41, 42] This implies that a PS-*b*-P4VP diblock copolymer will be in the strong segregation limit even for the diblock copolymers with lowest molecular weights in our study.

Table 1. Specifications of the investigated PS-*b*-P4VP diblock copolymers

PS-*b*-P4VP Sample name [a]	M_n total (kg/mol)	PDI	wt % PS	wt % P4VP	ϕ_{P4VP}	χN [b]
$PS_{75}P4VP_{25}^{100}$	100	1.05	75.0	25.0	0.253	336
$PS_{88}P4VP_{12}^{109}$	109	1.10	88.0	12.0	0.121	366
$PS_{83.7}P4VP_{16.3}^{113}$	113	1.06	83.7	16.3	0.164	380
$PS_{86.5}P4VP_{13.5}^{150}$	150	1.06	86.5	13.5	0.136	504
$PS_{88.7}P4VP_{17.3}^{154}$	154	1.06	82.7	17.3	0.174	517
$PS_{81}P4VP_{19}^{160}$	160	1.06	81.0	19.0	0.192	537
$PS_{81}P4VP_{19}^{167}$	167	1.06	81.0	19.0	0.192	561
$PS_{84.5}P4VP_{15.5}^{175}$	175	1.09	84.5	15.5	0.156	588
$PS_{74}P4VP_{26}^{184}$	184	1.38	74.0	26.0	0.263	618
$PS_{81.2}P4VP_{18.8}^{188}$	188	1.08	81.2	18.8	0.190	632
$PS_{82.8}P4VP_{17.2}^{190}$	190	1.08	82.8	17.2	0.173	638
$PS_{78}P4VP_{22}^{191}$	191	1.10	78.0	22.0	0.222	641
$PS_{88,2}P4VP_{11.8}^{193}$	193	1.09	88.2	11.8	0.119	649
$PS_{76}P4VP_{24}^{197}$	197	1.06	76.0	24.0	0.243	661
$PS_{87.3}P4VP_{16.3}^{197}$	197	1.06	83.7	16.3	0.164	662
$PS_{83.3}P4VP_{16.7}^{198}$	198	1.07	83.3	16.7	0.168	665
$PS_{91}P4VP_{9}^{214}$	214	1.10	91.0	9.0	0.090	720
$PS_{84}P4VP_{16}^{238}$	238	1.08	84.0	16.0	0.161	800
$PS_{79.8}P4VP_{20.2}^{252}$	252	1.10	79.8	20.2	0.204	846
$PS_{78}P4VP_{22}^{264}$	264	1.10	78.0	22.0	0.222	887
$PS_{74.4}P4VP_{25.6}^{270}$	270	1.06	74.4	25.6	0.259	906
$PS_{75.2}P4VP_{24.8}^{285}$	285	1.08	75.2	24.8	0.251	957
$PS_{74.8}P4VP_{25.2}^{300}$	300	1.40	74.8	25.2	0.255	1.007
$PS_{73.4}P4VP_{26.6}^{310}$	310	1.30	73.4	26.6	0.269	1.041
$PS_{76}P4VP_{24}^{330}$	330	1.30	76.0	24.0	0.243	1.108

[a] In the sample name, lower case numbers indicate the amount of the respective block in wt%, and upper case number indicates the total molecular weight in kg/mol

[b] χ is the Florry - Huggins interaction parameter: $\chi_{S,4VP} = 0.35$. [41, 42] and N is the degree of polymerization of the whole diblock copolymer.

3.2 Membrane Formation

In general the membrane formation could be divided into two steps: 1) the initiation by microphase separation, driven by the self-assembly tendency upon evaporation of solvent, followed by the propagation which is driven by the concentration gradient, and 2) finally from the fixation of the surface structure and precipitation of the highly swollen polymer by the

non-solvent – solvent exchange. It should be noted that a membrane formation by quenching from a highly concentrated solution leads to non-equilibrium states. The duration of the first step is crucial for the membrane formation and could be accurately controlled through the use of a custom made casting machine (**Figure 1**).

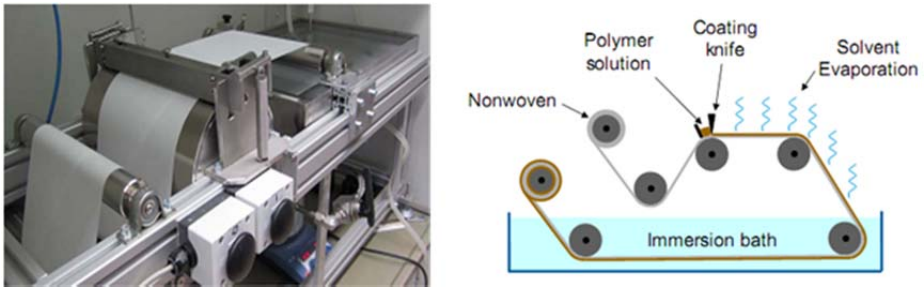

Fig. 1 Laboratory-size casting machine and the schematic representation of the operation principle.

Based on previously reported results[23] we chose solvent mixtures of THF and DMF. The more volatile THF is slightly selective for the PS blocks while the less volatile DMF is selective for the P4VP blocks, as it follows from the solubility parameters (**Table 2**).[43]
As known, block or graft copolymers are forming micelles in selective solvents that are good for one block (or grafts) and a non-solvent for the other.[44]
For PS-*b*-P4VP block copolymers, micellar aggregates are observed in the solution due to the incompatibility of the two polymer blocks. In a recent study on the same system Oss-Ronen et al. showed by cryo transmission and cryo scanning electron microscopy as well as by small angle neutron scattering that the copolymer forms micelles already in the casting solution. In particular the starting point for the membrane formation is a micellar block copolymer solution where the hydrophilic minor blocks (P4VP) are located within the micelle core. [29]
The Wiesner group found by small angle X-ray scattering that there is no structure formation at the polymer concentration in their casting solutions, but at slightly higher concentrations self-assembly takes place.[45] A similar conclusion for polystyrene-*block*-poly(ethylene oxide) in mixed solvents was drawn based on dynamic light scattering and turbidity measurements by our group.[46] Small angle X-ray scattering studies in casting solutions of PS-*b*-P4VP were recently presented giving rise to suspicion that the pore morphology is already incipient in the casting solution. These results were supported by cryo-FESEM, and modelling by dissipative particle dynamics demonstrated how the block copolymer self-assembly in solution, influenced by concentration and polymer–solvent interaction, can lead to the formation of regular pores in membranes.[47]

These works share in common that the casting solution should be at a concentration very close to the concentration dependent disorder-order transition. The P4VP chains are dissolved only in DMF and tend to precipitate into THF, while the dissolution of the PS chains is less favourable in DMF, but possible. The block copolymer concentration of each solution in our work is usually ranging from 20 to 30 wt %. Minor changes in the polymer concentration may lead to tremendous changes, as the viscosity and thus the mobility of the chains is affected. Micellar structures in the solution could be a good explanation for this system as well. After the block copolymer solution is cast, the THF is evaporating faster than DMF. At some stage, either microphase separation or a reorganisation of micellar structures will occur due to the increasing polymer concentration.[24] Furthermore this leads to a shrinking and solidification of the PS matrix, while the P4VP blocks remain strongly swollen by DMF.
By introducing this film into the precipitant (water) the already formed surface structure becomes frozen. Water exchanges through the more hydrophilic cylindrical P4VP domains at the surface by replacing DMF and precipitates the less organized block copolymer solution under the well-organized top layer. This leads to the well-known sponge-like substructure. Therefore, the resulting integral asymmetric structure is far from an equilibrium state.

Table 2 Hansen solubility parameters of homopolymers and solvents

Polymer	δ [$MPa^{0.5}$]	Solvent	δ [$MPa^{0.5}$]
PS	18.6	DMF	24.8
P4VP	22.2	THF	20.3

The precipitant and the solvent mixture used during the membrane preparation determine both the activity coefficient of the polymer at the point of precipitation and solidification. Several experiments to define the optimal waiting time prior to precipitation, to reach the desired surface structure, were conducted and are exemplary presented in **Figure 2**. Three major factors influence the membrane structure: solvent composition, polymer concentration, and evaporation time. They are assigned as axes in this depiction. **Figure 2** illustrates the structure formation on the surface of the membrane for a specific block copolymer $PS_{81}P4VP_{19}^{160}$ in dependence on the solvent composition and time prior to precipitation. For a solvent composition DMF/THF – 70/30 and for different times prior to precipitation (5-20 seconds) there was no pore formation observed (**Figure 2 a-d**). At this point we should note that for the same solvent composition, there was no regular pore structure on the membrane surface found for none of the diblock copolymers studied in this work. In the case of a solvent composition DMF/THF – 60/40 the best membrane was observed after 5 seconds, whereas with increasing

evaporation time the form and size of the pores became irregular (**Figure 2 e-h**). Further increasing of the THF content in the solution (50/50 **Figure 2 i-l** or 40/60 **Figure 2 m-p**) shifts the evaporation time to higher values in order to obtain the desired structure.

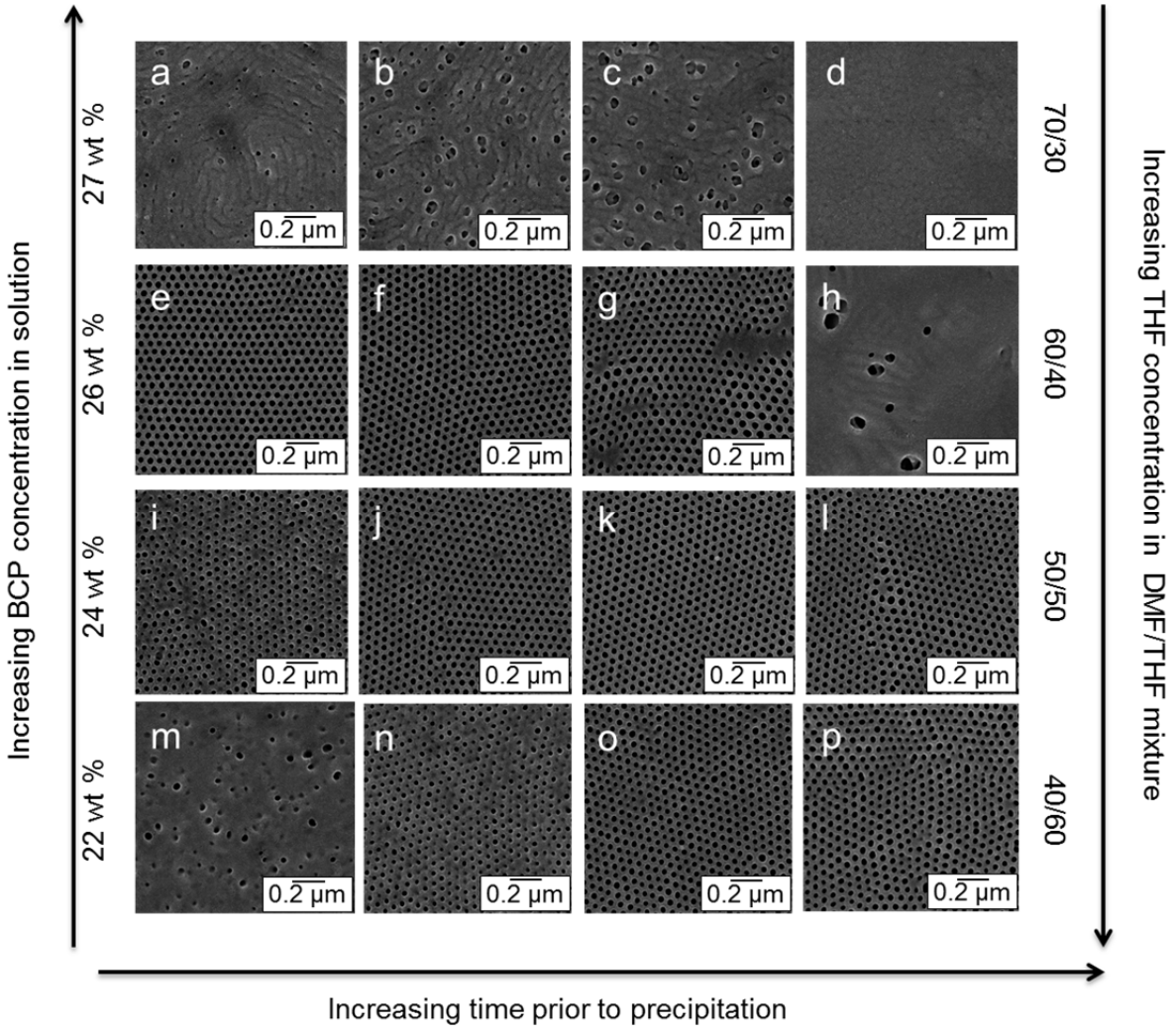

Fig. 2 SEM images of membrane surfaces. All membranes were cast from the same diblock copolymer $PS_{81}P4VP_{19}^{160}$. The time prior to precipitation varied in each case. (a-d) 27 wt % diblock copolymer in DMF/THF - 70/30 (e-h) 26 wt % diblock copolymer in DMF/THF - 60/40 (i-l) 24 wt % diblock copolymer in a DMF/THF - 50/50 (m-p) 22 wt % diblock copolymer in a DMF/THF - 40/60.

By increasing the THF content the solution viscosity is increasing due to the limited solubility of the P4VP-segments. In order to keep the solution capable of flowing it is essential to reduce the polymer concentration in the solution (**Table 3**). Less concentrated diblock copolymer solutions require longer evaporation times prior to precipitationin order to get the required polymer density on the membrane surface to form the desired porous structure. Thus, there is a strong relationship between the solvent composition and the evaporation time to

reach the desired surface structure.

Table 3. Solution characteristics leading to the membranes depicted in **Figure 2**

Polymer	Polymer conc. [wt %]	DMF/THF [wt %/wt %]	Dyn. Visc. [Pa*s]
PS_{81}-$P4VP_{19}^{160}$	22	40/60	0.8
PS_{81}-$P4VP_{19}^{160}$	24	50/50	1.1
PS_{81}-$P4VP_{19}^{160}$	26	60/40	1.4
PS_{81}-$P4VP_{19}^{160}$	27	70/30	1.4

In general solvent compositions DMF/THF - 60/40 and - 50/50, and short evaporation times of 5-10 s led to the optimum results for almost all block copolymers studied in this work. In **Figure 3** are presented indicative results of membrane surface structures from systematically increasing the total molecular weight of the diblock copolymers and their P4VP weight contents. The molecular weight was increased from 100 kg/mol up to 190 kg/mol, while the P4VP part was varied from 12 to 25 wt %. Diblock copolymers with a total molecular of approximately 105 kg/mol up to 195 kg/mol with approximate P4VP content 12 wt%, 17wt%, 19 wt%, and 24 wt% could be categorized into the following groups (a) approximately 12 wt% P4VP ($PS_{88}P4VP_{12}^{109}$, $PS_{86.5}P4VP_{13.5}^{150}$, and $PS_{88}P4VP_{12}^{193}$), (b) approximately 17 wt% P4VP ($PS_{83.7}P4VP_{16.3}^{113}$, $PS_{82.7}P4VP_{17.3}^{154}$, and $PS_{82.8}P4VP_{17.2}^{190}$), (c) approximately 19 wt% P4VP ($PS_{81}P4VP_{19}^{104}$, $PS_{81}P4VP_{19}^{160}$, and $PS_{81.2}P4VP_{18.8}^{188}$), (d) approximately 24 wt% P4VP ($PS_{75}P4VP_{25}^{100}$, $PS_{74}P4VP_{26}^{162}$, and $PS_{76}P4VP_{24}^{197}$). The casting solution characteristics and approximate pore sizes with the average pore size standard deviation of the resulting membranes are summarized in the **Table 4**.

Table 4. Conditions and average pore sizes of the membranes shown in **Figure 3**.

	M_n total (kg/mol)	$M_{n\ P4VP}$ (kg/mol)	wt % P4VP	Polymer Conc. [wt %]	DMF/THF [wt %/wt %]	Dynamic Viscosity [Pa s]	Average Pore Size* [nm]
Group 1 (Total M_n≈105 Kg/mol)							
$PS_{88}P4VP_{12}^{109}$	109	13	12.0	34.0	50/50	2.9	23±2
$PS_{83.7}P4VP_{16.3}^{113}$	113	18.5	16.3	32.0	50/50	2.1	23±2
$PS_{81}P4VP_{19}^{104}$	104	19.7	19.0	31.0	50/50	1.3	22±2
$PS_{75}P4VP_{25}^{100}$	100	25	25.0	27.0	50/50	0.5	25±2
Group 2 (Total M_n≈155 Kg/mol)							
$PS_{86.5}P4VP_{13.5}^{150}$	150	20.3	13.5	31.0	50/50	3.0	25±2
$PS_{82.7}P4VP_{17.3}^{154}$	154	26.6	17.3	27.0	60/40	1.6	30±3
$PS_{81}P4VP_{19}^{160}$	160	30.4	19.0	26.0	60/40	1.3	34±4

$PS_{74}P4VP_{26}^{162}$	162	42.1	26.0	24.0	60/40	0.6	38.±4
Group 3 (Total M_n≈195 Kg/mol)							
$PS_{88}P4VP_{12}^{193}$	193	23.2	12.0	-	-	-	-
$PS_{82.8}P4VP_{17.2}^{190}$	190	32.7	17.2	25.5	60/40	1.7	42±4
$PS_{81.2}P4VP_{18.8}^{188}$	188	35.3	18.8	25.0	60/40	1.2	44±4
$PS_{76}P4VP_{24}^{197}$	197	47.3	24.0	19.0	60/40	0.5	48±5

*The numeric value is attributed to the average pore diameter followed by the ± standard deviation

As seen in **Figure 3**, with the exception of block copolymer $PS_{88}P4VP_{12}^{193}$, for all other polymers the hexagonal porous structure on the membrane surface was achieved.

The membranes formed from higher molecular weight polymers with high P4VP content have larger pores and larger pore size dispersity (**Figure 3 c-d**). For membranes resulting from diblock copolymers containing 25 wt % P4VP connected pores were observed. An indicative example is a membrane made from the diblock copolymer with the highest molecular weight, $PS_{76}P4VP_{24}^{197}$. On the surface of this membrane we observe inhomogeneously sized pores and interconnected pores. The P4VP weight percentage is the highest from this group of diblock copolymers as well. The dissolution of this block will be limited in the solvent system of DMF/THF. In this case the longer polymer chains are hindered, due to their size, to self-assemble into uniform microphase separated structures within the given evaporation time. Diblock copolymers with lower molecular weights ($PS_{82.8}P4VP_{17.2}^{193}$, $PS_{81.2}P4VP_{18.8}^{188}$) and similar amounts of P4VP lead to membranes with homogenous surfaces, with narrower pore size distribution and fewer defects.

On the contrary, attempts to form membranes with a diblock copolymer of the same molecular weight and lower amount of P4VP, $PS_{88}P4VP_{12}^{193}$, failed, revealing a lower limit of the P4VP block to the total polymer composition at higher molecular weights. The reason for this is the low P4VP part in comparison with the total molecular weight. The solvent ratio was taken to all extremes in this case, but the formation of a porous membrane did not succeed. The long PS chains are probably well dissolved, while the P4VP chains are not able to segregate due to the insufficient time for self-assembly during the evaporation of THF. In terms of thermodynamics, the tendency to microphase separate should be much larger compared to block copolymers with same composition but lower molecular weights, thus the absence of an ordered structure formation is due to the lower mobility. A larger fraction of P4VP increases the enthalpic repulsion between the blocks and therefore also leads to a higher diffusivity of the blocks, as diffusivity is dependent on both the thermodynamic separation force and the mobility.

The membrane formation is strongly dependent on the structures formed in the solution. With increasing P4VP content a larger part of the diblock copolymer is collapsing due to the poor solubility of that block. After casting the diblock copolymer solution, THF is evaporating, and the PS micellar coronas are becoming less soluble in the solution, the chains are packing into the final morphology and their movement becomes highly restricted. The restriction of mobility of the chains will be more significant in the case of the large molecular weight diblock copolymers. On the contrary the P4VP chains are diluting into the rich in DMF solution and remain highly swollen up to the moment when the film is precipitated. At this point the already more solidified structure of the PS can further shrink, while the pore size is increasing as the P4VP chains are trying to place in a way reaching a low free enthalpy conformation (equilibrium). As an observation, the PS wall thickness appears to be rather unaffected by the molecular weight. As the molecular weight is increasing, pores with bigger diameters are observed. The increment of the pore size values is linear offering the opportunity of controllable or predictable pore size formation. As described above, the membrane formation is strongly influenced by the polymeric structures formed in the micellar solutions prior to the membrane formation. Lower molecular weight block copolymers are expected to lead to smaller micellar assemblies than the higher molecular weights with equivalent amount of P4VP. As summarized in **Table 4** the average pore diameters are increasing gradually from ca. 22 nm to ca. 34 nm and finally reaching approximately 44 nm. The average pore size diameters are increasing linearly with the total molecular weight and in particular by doubling the molecular weight a doubling in the average pore size is achieved.

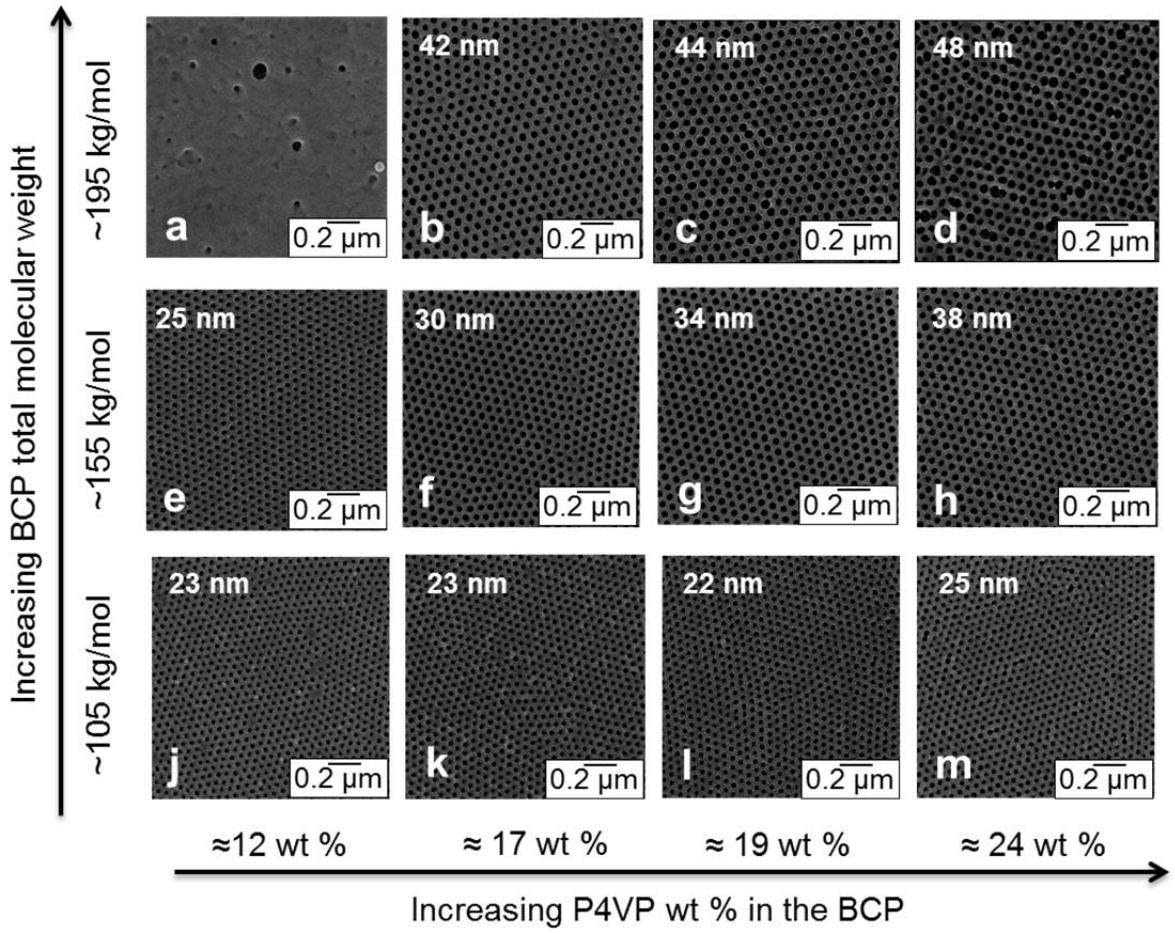

Fig.3 SEM images from integral asymmetric membranes of a series of polymers studied on their ability of forming integral asymmetric membranes. Both an increase of the P4VP block length in the block copolymer or a higher block copolymer total molecular weight lead to enlargement of the pore diameters.

The increment is linear in all cases and this can be also observed when the membrane average pore sizes are plotted as a function of the total molecular weight (**Figure 4**).

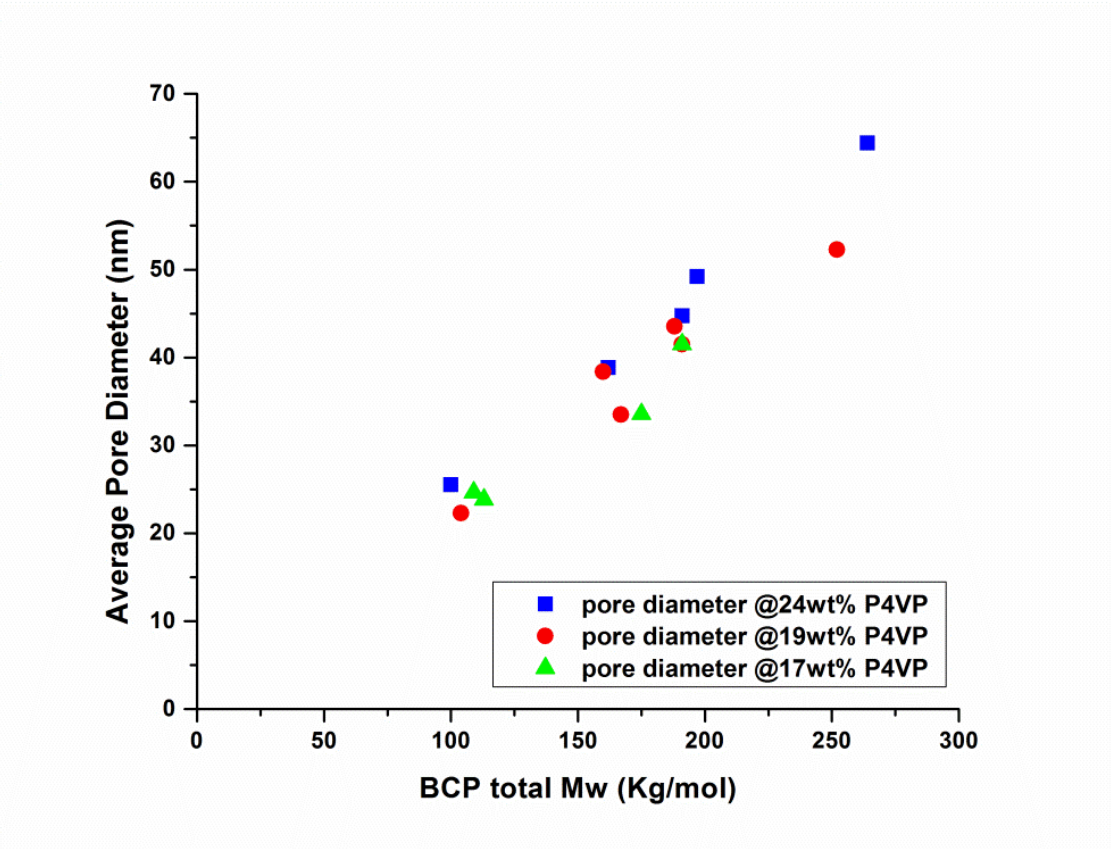

Fig.4 Plot of average pore diameter versus the total molecular weight of the diblock copolymer, for different amounts of P4VP.

Interesting conclusions could also be drawn from the third group of diblock copolymers of this study which include the polymers with molecular weights of approximately 195 Kg/mol having different P4VP wt% contents. In particular these are the polymers $PS_{88}P4VP_{12}$[193], $PS_{82.8}P4VP_{17.2}$[193], $PS_{81.2}P4VP_{18.8}$[188], and $PS_{76}P4VP_{24}$[197], respectively. The average pore size is not changing significantly, but the polydispersity of the pore sizes and the shape of the pores are affected significantly. In general the higher molecular weight diblock copolymers lead to membranes with increased pore size distribution. In all cases the viscosity of the solutions was monitored via rotational viscometry and the results are listed in **Table 3**. The micellization into the typical “core” / “corona” micelles in amphiphilic block copolymers in a solution is beginning upon the critical micelle concentration and evolving into lyotropic structures as the solution concentration in block copolymer is increasing. Viscosity is one of the key indicators of the solution’s potential to form porous membranes, as it is indicative for hydrodynamic properties of the micellar aggregates. The micellar aggregates are formed by the less soluble P4VP core and the PS corona, and they depend on the ratio between the two blocks. When the P4VP block is small, relatively high concentrations (30 % wt) are required, so that micellar structures can lead to the formation of well-ordered porous structures on the membrane

surface. For higher P4VP weight ratios the micellar aggregates are formed at lower required polymer concentrations since then the non-soluble part is longer and leads to a lower solubility. The total molecular weight of the block copolymer and composition are affecting the required polymer concentration (**Table 3**). The solution viscosity appears to be more influenced by the P4VP weight ratio and less by the molecular weight of the block copolymer. In **Figure 5** the rotational viscosity is plotted as a function of the amount of P4VP in the block copolymer, following a non-linear decrease.

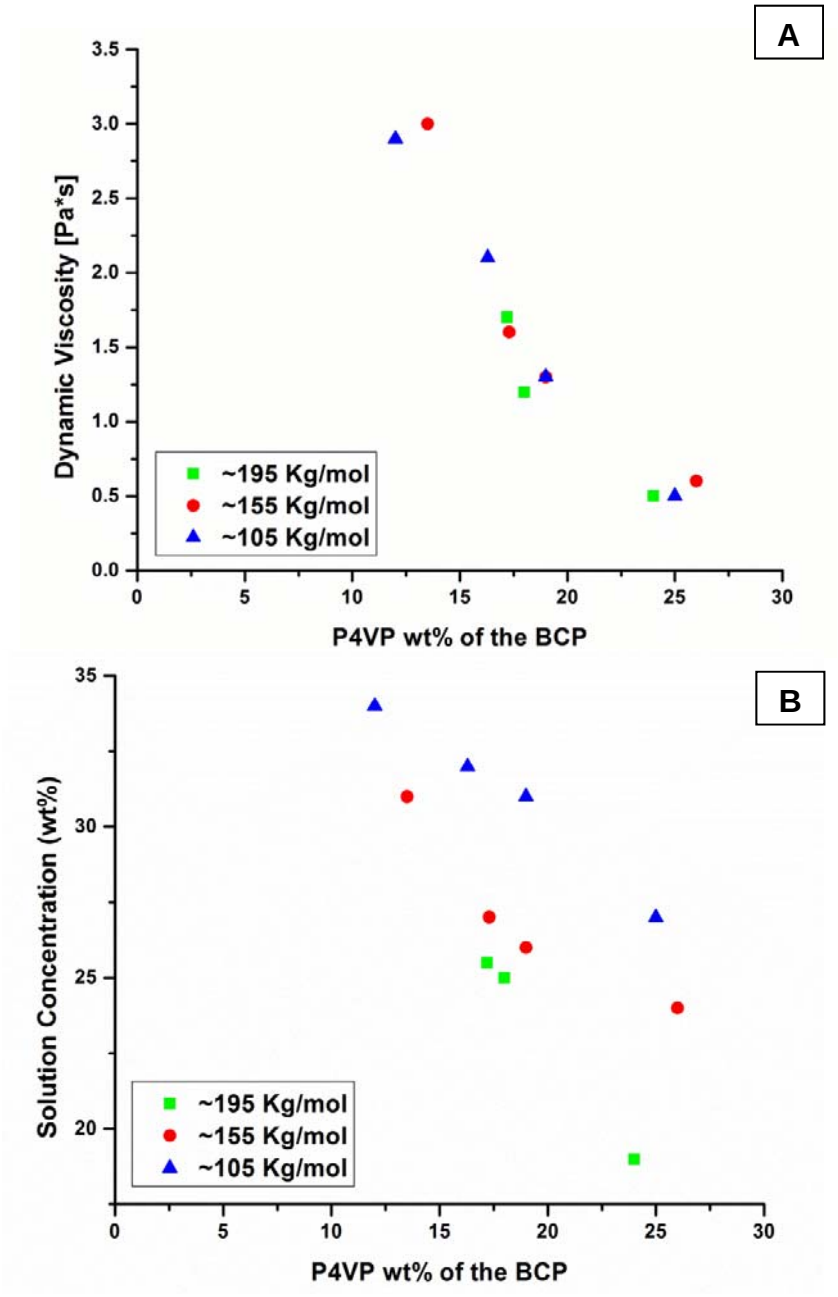

Fig.5 Plots of (A) dynamic viscosity and (B) solution concentration versus the content of P4VP in the PS-*b*-P4VP diblock copolymers.

When the P4VP content in the block copolymer is increasing, the amount of material needed to achieve a solution viscosity that will lead to successful membranes is less. Increased viscosity of the initial solution leads to an increased pore size polydispersity as well (**Figure 3d**).

The polymer concentration in the casting solution has a significant effect on the membrane body structure. As it is described in the literature, when the polymer concentration in the casting solution is low, there is a tendency of the structure to precipitate in a finger structure (cylindrical pores), while high polymer concentrations tend to form sponge structure membranes (sponge-like pores)[7]. The effect of polymer concentration on the membrane structure can be explained by the initiation and propagation of the cylindrical pores. The higher polymer concentration in the casting solution tends to prevent initiation of them due to the restricted mobility of the polymeric chains leading to membranes with sponge like structures on the membrane body, but well defined hexagonal porous structures on the membrane surface. In **Figure 6** the indicative cross sections of two different membranes with the same total molecular weight but different amounts of P4VP are presented. The increasing viscosity of a casting solution has the same effect, as the movement of the polymeric chains is restricted due to the higher amount of polymer. The dynamic viscosity of the polymeric solution with 24 wt % was 1.1 Pa s (Figure 7 left image), while for the 26 wt % polymeric solution the dynamic viscosity value was 1.4 Pa s (Figure 7 right image).

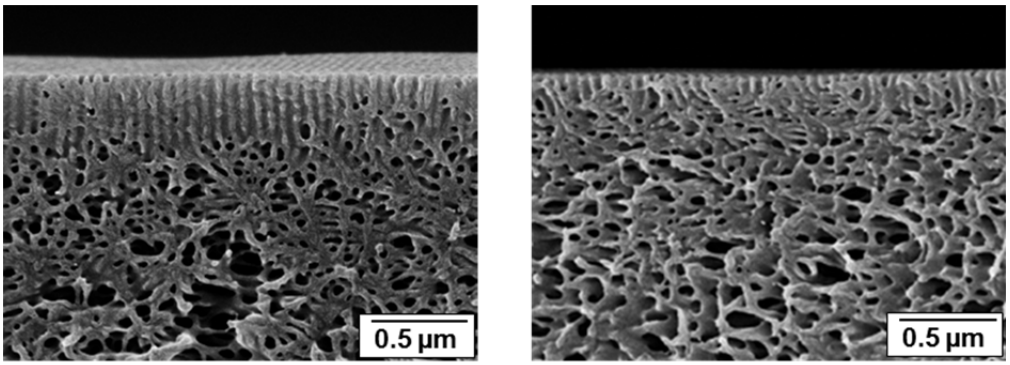

Fig.6 Cross sections from two different block copolymer membranes. The left image shows the cross section of a $PS_{74}P4VP_{26}^{160}$ membrane cast from a 24 wt % solution in a DMF/THF-60/40 w/w solvent mixture. The right image is a cross section of a $PS_{81}P4VP_{19}^{160}$ membrane cast from a 26 wt % solution in a DMF/THF-60/40 w/w solvent mixture. Time prior to precipitation was 10 seconds.

3.3 Water flux and retention measurements

The control of the pore size and high porosity of these membranes (around 40%) are making them ideal candidates for size selective separation processes. Two membranes from different molecular weight diblock copolymers but having the same P4VP wt% were tested by pure water flux measurements. The average pore size of the first membrane was 38 nm and the flux curve is shown in **Figure 7** (red squares). The maximum of the flux is about 625 L / (h·m^2·bar). The flux curve of the second membrane (**Figure 7**, blue circles) shows a maximum value of flux at 450 L / (h·m^2·bar) while the average pore size in this case was 25 nm.

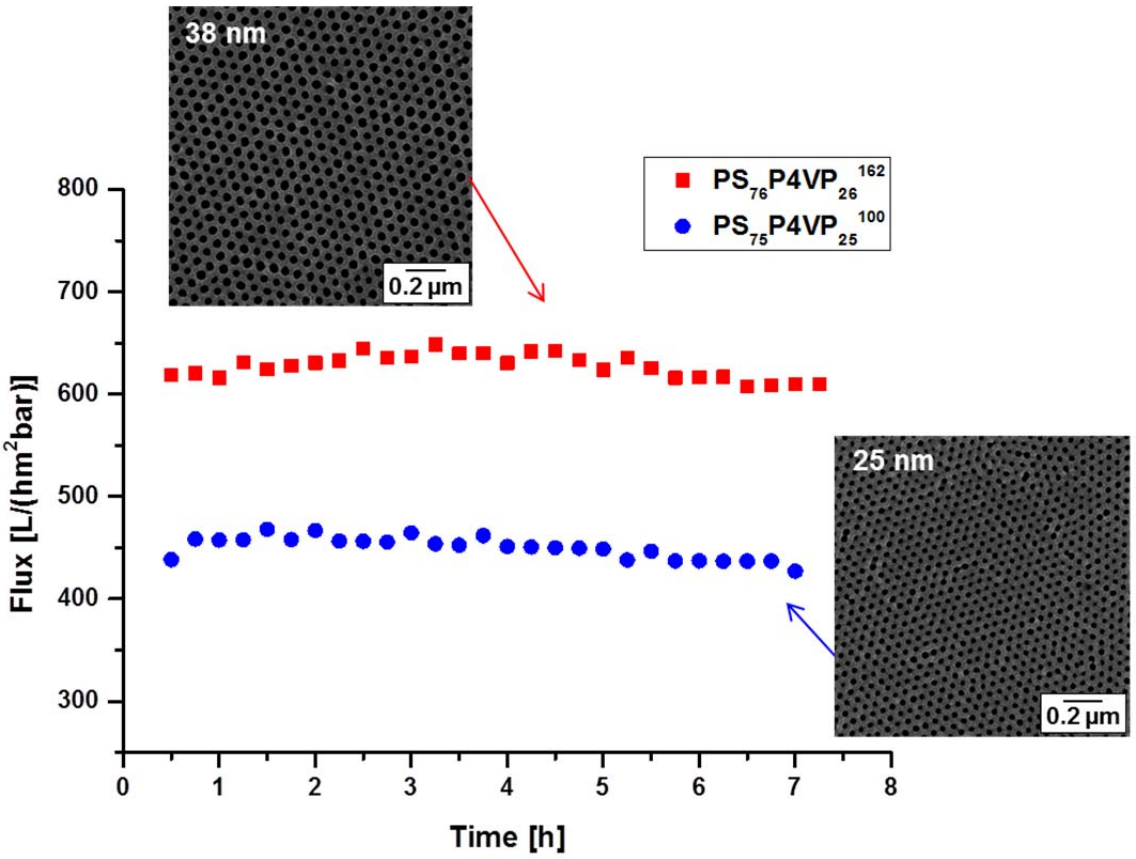

Fig. 7: Pure water flux of two PS-*b*-P4VP membranes with different pore size. red squares: flux results from the membrane with 38 nm average pore size and blue circles: flux results from the membrane with 25 nm average pore size.

This is a first indication that the membrane flux properties could follow a trend in terms of the pore sizes on the membrane top layer. The flux properties as a function of the membrane structure are a subject of on-going studies.

In order to evaluate the experimentally investigated water flux value (i.e. at open pore conditions of the membrane) the Hagen-Poiseuille law for a laminar flow in simple straight cylinders was applied. This appears justified, if the top layer of cylinders in the membrane structure is based on a spongy, rather open structure with larger porosity, i.e. if the flux is mainly hindered by the top layer itself:

$$\dot{V} = \frac{\pi \cdot r_{pore}^4 \cdot \Delta p}{8 \cdot \eta \cdot L} \quad (1)$$

with V: water flux; r_{pore} : radius of open pore; Δp: pressure drop; η: viscosity of water (8.94×10^{-4} Pa*s at 24°C)[48]; L : length of open pore. Both membranes cross sections are depicted in Figure 8. In Figure 8A the $PS_{74}P4VP_{26}^{160}$ membrane is shown, having an average pore diameter of 38 nm and pore length of approximately 130 nm**.** The expected water flux value according to the Hagen-Poiseuille law for the membrane characteristics and the trans membrane pressure of 2.1 bar is approximately 39160 L / (m^2·h·bar). In the case of the second membrane ($PS_{75}P4VP_{25}^{100}$) with 25 nm pore diameter and 120 nm pore length(**Figure 8B)**, the theoretically calculated water flux from equation (1) is 12805 L / (m^2·h·bar). In **Table 5** the theoretical and experimental flux values, the average pore diameter, the average pore length, and the average number of pores per m^2 are given.

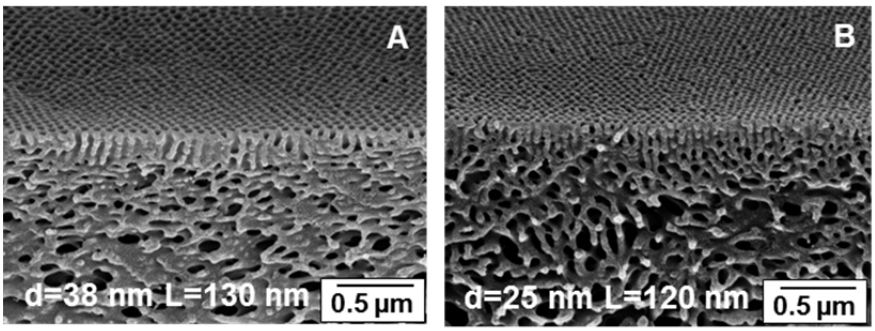

Fig.8 Cross sections from the two different block copolymer membranes shown in Figure 7. (A) the cross section of a $PS_{74}P4VP_{26}^{160}$ membrane having an average pore diameter of 38 nm and pore length of approximately 130 nm. (B) the cross section of a $PS_{75}P4VP_{25}^{100}$ membrane having an average pore diameter of 25 nm and pore length of approximately 120 nm.**Table 5**: Membrane characteristics used in the Hagen-Poiseuille equation (1), theoretical and experimental water flux values

Membrane	Average Pore Diameter [nm]	Average Pore Length [nm]	Average Pore Number per m^2	Theoretical Water Flux[1] [L/ m^2·h·bar)]	Experimental Water Flux[2] [L/(m^2·h·bar)]
$PS_{75}P4VP_{25}^{100}$	25	120	3.98×10^{14}	12805	450
$PS_{74}P4VP_{26}^{160}$	38	130	2.47×10^{14}	39160	625

[1]The values are calculated used the equation (1) for a membrane area of 1 m^2 and trans membrane pressure 2.1 bar[2]Actual flux as calculated during clean water flux experiments for a trans membrane pressure 2.1 bar

As specified above, the equation (1) describes the laminar flow of a liquid through a simple straight cylinder. For this reason the deviation of the experimentally measured flux from the theoretical values is tremendous, as water is a highly associated liquid with these type of membranes. The P4VP chains swell in water, the pore diameter is decreasing reducing the flux, similarly to the description of flux behavior from PS-*b*-P2VP block copolymer membranes.[24] Calculating backwards to estimate the size of the pores that would lead to the experimentally observed flux values, the pore diameter of the $PS_{74}P4VP_{26}^{160}$ membrane is 13.5 nm [experimental water flux: 625 L / (m^2·h·bar)], and for the $PS_{75}P4VP_{25}^{100}$ membrane it is 10.8 nm [experimental water flux: 450 L / (m^2·h·bar)].

Moreover from a look onto the SEM images of the depicted cross sections in Figure 8, the supportive spongy layer of the integral asymmetric membrane shows areas of large pores and also areas of rather dense, curved pores expected to increase the resistance to the flow. Thus a better description of the theoretical value for this system flux value should include a factor of the flow resistance by also considering the tortuosity of the supportive layer, which is difficult to be determined.

The first results concerning the separation properties of PS-b-P4VP membranes with different pore sizes indicate big differences between their retention characteristics. All retention measurements were carried out using a 0.05 wt % BSA solution in water. Indicative are given the results of a membrane made from the $PS_{83.7}P4VP_{16.3}^{113}$ block copolymer (pore diameter ≈23 nm) exhibiting a 90 % retention of BSA with a flux of 50 L / (m^2·h·bar) during retention measurements. A membrane made from $PS_{78}P4VP_{22}^{191}$ (pore diameter ≈ 42 nm) had only a 17 % retention capacity with a flux of 240 L / (m^2·h·bar) during retention experiment. Using an even higher molecular weight by the membrane formation a $PS_{78}P4VP_{22}^{264}$ diblock copolymer, retention of 5 % was measured with a flux of 390 L / (m^2·h·bar) during the experiments. The results are summarized in **Table 6**.

Table 6: Retention results from experiments in a 0.05 wt % BSA solution in water

Membrane	Average Pore Diameter [nm]	Flux [L/(m^2·h·bar)]	% BSA retention
$PS_{83.7}P4VP_{16.3}^{113}$	23	50	90
$PS_{78}P4VP_{22}^{191}$	42	240	17
$PS_{78}P4VP_{22}^{264}$	68	390	5

The retention properties of these membranes need to be further investigated using different types of retendants. As the hydrodynamic diameter of BSA is much below the pore size, the retention of it depends probably mostly on the interaction with the membrane, rather than being a size effect.[24] A detailed examination of the separation characteristics of the different membranes and retendants is still in progress.

4. Conclusion

The formation of isoporous membranes from block copolymer membranes through the combination of self-assembly and the non-solvent induced phase separation of amphiphilic polystyrene-*block*-poly(4-vinylpyridine) diblock copolymers with various molecular weights and block lengths was attempted. SEM investigations were carried out in order to check the homogeneity, average pore size and pore size distribution. By examining several PS-*b*-P4VP diblock copolymers with different molecular characteristics an improved understanding of the formation mechanism of the porous structure was achieved. Upon the evaporation of THF after casting of the initial solution, the coronas of the micellar aggregations (PS blocks) are beginning to solidify forming the matrix of the isoporous structure on the membrane surface. Simultaneously the system is driven towards a transition from spherical micelles to cylindrical structure at the membrane surface before being immersed into the precipitation bath, as the effective volume fraction of the swollen polystyrene coronas, which are originally richer in THF, decreases. The membrane formation (porous network on the membrane body) is completed upon the exchange of solvent by non-solvent when the cast film is entering the precipitation bath. The highly swollen P4VP blocks precipitate within the previously mixed P4VP/DMF domains upon the exchange of DMF by water. In case of higher molecular weight polymers the chain movement is already hindered by the increased number of entanglements and chain length, thus kinetically more stable micellar aggregates are formed. On the other

hand the membrane formation from lower molecular weight block copolymers is strongly depending on the solution viscosity. Systematic studies on the solution viscosities revealed that the higher P4VP block length is affecting more the overall solution viscosity, than the increment of the block copolymer total molecular weight. For P4VP block weight ratios more than 25 wt % SEM studies revealed inhomogeneous pore sizes and more defects on the membrane surface.

Morphological studies from membranes made from solutions of diblock copolymers with a total molecular weight of about 190 kg/mol revealed a lower limit in the P4VP block. This limit was not found for block copolymers with lower molecular weights since in this case the movement hindrance of the blocks is not as large, allowing the micellar structures to evolve.

Though the pore diameters are in accordance with a linear function of the molecular weight of the investigated block copolymers, the pore wall thickness on the contrary is not following a similar function. In this case a function dependent to the polymer concentration seems to be followed. The length of the cylindrical channels is shorter when the polymer solution viscosity is increasing.

In general smaller pore sizes result in smaller water fluxes. Also retention increases with decreasing pore sizes, but require further investigations.

Acknowledgements

The authors acknowledge Silvio Neumann, Clarissa Abetz, Sabrina Bolmer, Anne Schroeder and Petra Merten for their help with NMR, SEM measurements and retention experiments respectively. This work is financially supported by FP7 EU-project SELFMEM under grant agreement NMP3-SL-2009-228652.

References

[1] Z. Wang, X. Yao, Y. Wang, Swelling-induced mesoporous block copolymer membranes with intrinsically active surfaces for size-selective separation, Journal of Materials Chemistry, 22 (2012) 20542-20548.

[2] F.S. Bates, G.H. Fredrickson, Block Copolymers—Designer Soft Materials, Phys Today, 52 (1999) 32.

[3] W. Yave, Membranes from Block Copolymers, Bentham Science Publishers 2012.

[4] S.P. Nunes, A. Car, From Charge-Mosaic to Micelle Self-Assembly: Block Copolymer Membranes in the Last 40 Years, Industrial & Engineering Chemistry Research, 52 (2013) 993-1003.

[5] P. Apel, Track etching technique in membrane technology, Radiat Meas, 34 (2001) 559-566.

[6] M. Hillmyer, Nanoporous Materials from Block Copolymer Precursors, in: V. Abetz (Ed.) Block Copolymers II, Springer Berlin Heidelberg, 2005, pp. 137-181.

[7] H. Strathmann, K. Kock, The formation mechanism of phase inversion membranes, Desalination, 21 (1977) 241-255.

[8] E.B. Zhulina, O.V. Borisov, Theory of Block Polymer Micelles: Recent Advances and Current Challenges, Macromolecules, 45 (2012) 4429-4440.

[9] J.N. Israelachvili, Intermolecular and Surface Forces, Academic Press, London, 1991.

[10] R.C. Hayward, D.J. Pochan, Tailored Assemblies of Block Copolymers in Solution: It Is All about the Process, Macromolecules, 43 (2010) 3577-3584.

[11] A. Desjardins, T.G.M. Van de Ven, A. Eisenberg, Colloidal properties of block ionomers. 2. Characterization of reverse micelles of styrene-b-methacrylic acid and styrene-b-metal methacrylate diblocks by dynamic light scattering, Macromolecules, 25 (1992) 2412-2421.

[12] Z. Gao, S.K. Varshney, S. Wong, A. Eisenberg, Block Copolymer "Crew-Cut" Micelles in Water, Macromolecules, 27 (1994) 7923-7927.

[13] A. Desjardins, A. Eisenberg, Colloidal properties of block ionomers. 1. Characterization of reverse micelles of styrene-b-metal methacrylate diblocks by size-exclusion chromatography, Macromolecules, 24 (1991) 5779-5790.

[14] R. Xu, Y. Hu, G. Riess, M.D. Croucher, M.A. Winnik, Study of polystyrene-poly(ethylene oxide) block copolymer micelles in aqueous solution by size-exclusion chromatography, Journal of Chromatography A, 547 (1991) 434-438.

[15] D.E. Discher, A. Eisenberg, Polymer vesicles, Science, 297 (2002) 967-973.

[16] R. Xu, M.A. Winnik, G. Riess, B. Chu, M.D. Croucher, Micellization of polystyrene-poly(ethylene oxide) block copolymers in water. 5. A test of the star and mean-field models, Macromolecules, 25 (1992) 644-652.

[17] K. Kazunori, K. Glenn S, Y. Masayuki, O. Teruo, S. Yasuhisa, Block copolymer micelles as vehicles for drug delivery, Journal of Controlled Release, 24 (1993) 119-132.

[18] R. Gref, Y. Minamitake, M.T. Peracchia, V. Trubetskoy, V. Torchilin, R. Langer, Biodegradable long-circulating polymeric nanospheres, Science, 263 (1994) 1600-1603.

[19] C. Allen, Y. Yu, D. Maysinger, A. Eisenberg, Polycaprolactone-b-poly(ethylene oxide) block copolymer micelles as a novel drug delivery vehicle for neurotrophic agents FK506 and L-685,818, Bioconjugate chemistry, 9 (1998) 564-572.

[20] D.H. Han, X. Tong, Y. Zhao, Fast Photodegradable Block Copolymer Micelles for Burst Release, Macromolecules, 44 (2011) 437-439.

[21] J.Z. Du, L. Fan, Q.M. Liu, pH-Sensitive Block Copolymer Vesicles with Variable Trigger Points for Drug Delivery, Macromolecules, 45 (2012) 8275-8283.

[22] E.A. Jackson, M.A. Hillmyer, Nanoporous membranes derived from block copolymers: from drug delivery to water filtration, ACS nano, 4 (2010) 3548-3553.

[23] K.V. Peinemann, V. Abetz, P.F. Simon, Asymmetric superstructure formed in a block copolymer via phase separation, Nature materials, 6 (2007) 992-996.

[24] A. Jung, S. Rangou, C. Abetz, V. Filiz, V. Abetz, Structure Formation of Integral Asymmetric Composite Membranes of Polystyrene-block-Poly(2-vinylpyridine) on a Nonwoven, Macromol Mater Eng, 297 (2012) 790-798.

[25] J. Hahn, V. Filiz, S. Rangou, B. Lademann, K. Buhr, J.I. Clodt, A. Jung, C. Abetz, V. Abetz, PtBS-b-P4VP and PTMSS-b-P4VP Isoporous Integral-Asymmetric Membranes with High Thermal and Chemical Stability, Macromol Mater Eng, (2013) n/a-n/a.

[26] S.P. Nunes, R. Sougrat, B. Hooghan, D.H. Anjum, A.R. Behzad, L. Zhao, N. Pradeep, I. Pinnau, U. Vainio, K.-V. Peinemann, Ultraporous Films with Uniform Nanochannels by Block Copolymer Micelles Assembly, Macromolecules, 43 (2010) 8079-8085.

[27] S.P. Nunes, M. Karunakaran, N. Pradeep, A.R. Behzad, B. Hooghan, R. Sougrat, H. He, K.-V. Peinemann, From Micelle Supramolecular Assemblies in Selective Solvents to Isoporous Membranes, Langmuir, 27 (2011) 10184-10190.

[28] S.P. Nunes, A.R. Behzad, B. Hooghan, R. Sougrat, M. Karunakaran, N. Pradeep, U. Vainio, K.V. Peinemann, Switchable pH-responsive polymeric membranes prepared via block copolymer micelle assembly, ACS nano, 5 (2011) 3516-3522.

[29] L. Oss-Ronen, J. Schmidt, V. Abetz, A. Radulescu, Y. Cohen, Y. Talmon, Characterization of Block Copolymer Self-Assembly: From Solution to Nanoporous Membranes, Macromolecules, 45 (2012) 9631-9642.

[30] M. Gallei, S. Rangou, V. Filiz, K. Buhr, S. Bolmer, C. Abetz, V. Abetz, The Influence of Magnesium Acetate on the Structure Formation of Polystyrene-block-poly(4-vinylpyridine)-Based Integral-Asymmetric Membranes, Macromolecular Chemistry and Physics, 214 (2013) 1037-1046.

[31] J.I. Clodt, S. Rangou, A. Schroder, K. Buhr, J. Hahn, A. Jung, V. Filiz, V. Abetz, Carbohydrates as additives for the formation of isoporous PS-b-P4VP diblock copolymer membranes, Macromolecular rapid communications, 34 (2013) 190-194.

[32] J.I. Clodt, V. Filiz, S. Rangou, K. Buhr, C. Abetz, D. Höche, J. Hahn, A. Jung, V. Abetz, Double Stimuli-Responsive Isoporous Membranes via Post-Modification of pH-Sensitive Self-Assembled Diblock Copolymer Membranes, Advanced Functional Materials, 23 (2013) 731-738.

[33] M. Radjabian, J. Koll, K. Buhr, U.A. Handge, V. Abetz, Hollow fiber spinning of block copolymers: Influence of spinning conditions on morphological properties, Polymer, 54 (2013) 1803-1812.

[34] P. Madhavan, K.-V. Peinemann, S.P. Nunes, Complexation-Tailored Morphology of Asymmetric Block Copolymer Membranes, ACS Applied Materials & Interfaces, (2013).

[35] S.Y. Yang, J. Park, J. Yoon, M. Ree, S.K. Jang, J.K. Kim, Virus Filtration Membranes Prepared from Nanoporous Block Copolymers with Good Dimensional Stability under High Pressures and Excellent Solvent Resistance, Advanced Functional Materials, 18 (2008) 1371-1377.

[36] M.M. Pendergast, R. Mika Dorin, W.A. Phillip, U. Wiesner, E.M.V. Hoek, Understanding the structure and performance of self-assembled triblock terpolymer membranes, Journal of Membrane Science, 444 (2013) 461-468.

[37] A. Jung, V. Filiz, S. Rangou, K. Buhr, P. Merten, J. Hahn, J. Clodt, C. Abetz, V. Abetz, Formation of integral asymmetric membranes of AB diblock and ABC triblock copolymers by phase inversion, Macromolecular rapid communications, 34 (2013) 610-615.

[38] X. Qiu, H. Yu, M. Karunakaran, N. Pradeep, S.P. Nunes, K.V. Peinemann, Selective separation of similarly sized proteins with tunable nanoporous block copolymer membranes, ACS nano, 7 (2013) 768-776.

[39] W.A. Phillip, M.A. Hillmyer, E.L. Cussler, Cylinder Orientation Mechanism in Block Copolymer Thin Films Upon Solvent Evaporation, Macromolecules, 43 (2010) 7763-7770.

[40] S.H. Kim, M.J. Misner, T. Xu, M. Kimura, T.P. Russell, Highly Oriented and Ordered Arrays from Block Copolymers via Solvent Evaporation, Advanced Materials, 16 (2004) 226-231.

[41] G.O.R. Alberda van Ekenstein, R. Meyboom, G. ten Brinke, O. Ikkala, Determination of the Flory−Huggins Interaction Parameter of styrene and 4-Vinylpyridine Using Copolymer Blends of Poly(styrene-co-4-vinylpyridine) and Polystyrene, Macromolecules, 33 (2000) 3752-3756.

[42] W. Zha, C.D. Han, D.H. Lee, S.H. Han, J.K. Kim, J.H. Kang, C. Park, Origin of the Difference in Order−Disorder Transition Temperature between Polystyrene-block-poly(2-vinylpyridine) and Polystyrene-block-poly(4-vinylpyridine) Copolymers, Macromolecules, 40 (2007) 2109-2119.

[43] J.I. Brandrup, E.A. Edmund H.; Grulke, A. Abe, D.R. Bloch, Polymer handbook, John Wiley & Sons, (1999) 675.

[44] G. Riess, Micellization of block copolymers, Progress in Polymer Science, 28 (2003) 1107-1170.

[45] R.M. Dorin, D.S. Marques, H. Sai, U. Vainio, W.A. Phillip, K.V. Peinemann, S.P. Nunes, U. Wiesner, Solution Small-Angle X-ray Scattering as a Screening and Predictive Tool in the Fabrication of Asymmetric Block Copolymer Membranes, Acs Macro Lett, 1 (2012) 614-617.

[46] J. Hahn, V. Filiz, S. Rangou, J. Clodt, A. Jung, K. Buhr, C. Abetz, V. Abetz, Structure formation of integral-asymmetric membranes of polystyrene-block-Poly(ethylene oxide), Journal of Polymer Science Part B: Polymer Physics, 51 (2013) 281-290.

[47] D.S. Marques, U. Vainio, N.M. Chaparro, V.M. Calo, A.R. Bezahd, J.W. Pitera, K.-V. Peinemann, S.P. Nunes, Self-assembly in casting solutions of block copolymer membranes, Soft Matter, 9 (2013) 5557-5564.

[48] J. Kestin, M. Sokolov, W.A. Wakeham, Viscosity of liquid water in the range -8 [degree]C to 150 [degree]C, Journal of Physical and Chemical Reference Data, 7 (1978) 941-948.